

COMPARISONS BETWEEN STEADY STATE ANALYSES OF A HIGH SWIRL-GENERATING HELICAL INTAKE PORT FOR DIESEL ENGINES

Mirko Baratta, mirko.baratta@polito.it
Andrea E Catania, andrea.catania@polito.it
Francesco C Pesce, francesco.pesce@polito.it
Ezio Spessa, ezio.spessa@polito.it
IC Engines Advanced Laboratory, Politecnico di Torino, Italy

Charles Rech, charlesrech@uol.com.br
Horácio A. Vielmo, vielmoh@mecanica.ufrgs.br
Department of Mechanical Engineering, Federal University of Rio Grande do Sul, Brazil

Abstract. A well known method to characterize intake systems of internal combustion engines is based on steady flow tests, with fixed pressure drops across the system at different valve lifts. A discharge coefficient is defined, which describes the breathing capacity of the intake system. The inlet port of the considered engine is a shallow ramp helical type, coupled with an inner seat valve diameter of 31.5 mm and outer of 34.5 mm, with bore of 79.5 mm and a stroke of 86 mm. However, in order to simulate the workbench, this last dimension was extended to 160 mm, compounding the whole calculus dominium. The maximum intake valve lift is 8.1 mm. Its discharge coefficient is analyzed, based on numerical solutions using the Fluent 6.3 commercial Finite Volumes CFD code. The simulations are performed and compared with experimental results, and also with Star_CD 3.26 commercial Finite Volumes CFD code solutions, presented in another paper. Regarding the turbulence, computations are performed with the Reynolds-Averaged Navier-Stokes, Eddy Viscosity Models $k-\epsilon$, in its High-Reynolds approach. The RNG variant was also tested. A detailed mesh independence study was performed, arriving in a submillimeter mesh of 523000 tetra-prism cells, including an extrusion layer of 0.02 mm, to assure an adequate wall treatment. The simulations were done for various intake and in-cylinder pressures. The enthalpy equation is also solved, and the air compressibility is considered, being treated as a perfect gas. The presence of recirculations in the port and in-cylinder are detected and discussed.

Keywords: discharge coefficient, CFD simulations, turbulence models, helical intake port, CI engines.

1. INTRODUCTION

The discharge coefficient in a Diesel internal combustion engine is studied computationally to assess the capability of Computational Fluid Dynamics (CFD) in assisting experimental calibration. This paper focuses on a steady state regime that occurs in the flow permeability tests of a Diesel engine intake system (CRF, Fiat Research Center; 1982, 1983).

The steady flow data are representative of the dynamic flow behavior of the valve in an operating engine. The pressure upstream of the valve varies significantly during the intake process. However, it has been shown that over the normal engine speed range, steady flow discharge coefficient results can be used to predict dynamics performance with reasonable precision (Heywood, 1988).

During the last years more numerical simulations have been done regarding the discharge coefficient (Bianchi et al., 2002, 2003), focusing in directed intake port types, including comparisons with experimental measurements. With the growing availability of turbulent models and computational resources, many works make comparisons, regarding their capacity of reproduce experimental data and CPU time demanding.

Kaario et al. (2003) compared the $k-\epsilon$ RNG turbulence model with the one-equation subgrid scale model, incompressible and isothermal LES approach (Large Eddy Simulation). This particularized form of the LES model used was able to capture more flow's complex structures than the $k-\epsilon$ RNG model ($k-\epsilon$ Renormalization Group), but remains the CPU large time demand problem.

Keeping the popular $k-\epsilon$ family, some works have been analyzing the alternatives for the stress-strain relationship, considering the compressible, non-isothermal, anisotropic effects presents in the ICE (Internal Combustion Engine) three-dimensional flows. Bianchi et al. (2002, 2003) compared $k-\epsilon$ linear and nonlinear (quadratic and cubic) eddy viscosity models, concluding that cubic stress-strain relation provided the best agreement with data, for those ICE three-dimensional flows considered. In another work (2003) the same authors investigated the High Reynolds and Low Reynolds near wall approaches, both with a cubic relationship between Reynolds stresses and strains. It was concluded that the Low Reynolds approach (boundary layer also discretized by the mesh), although increasing the computational effort, presented more ability in capturing the tested ICE intake flow.

An alternative is to use *RNG* models instead of nonlinear ones, considering its underlying concepts similar to non linear models, but with more objective simplicity. Baratta et al. (2003) obtained a better experimental agreement for engine flows modifying the *RNG* constants, presenting another valid possibility.

The present work reports a comparison between experiments and simulations results of a discharge coefficient in an intake port of diesel engine to three valve lift different.

2. EXPERIMENTAL DATA

The inlet port of the considered engine is a shallow ramp helical type, coupled with an inner seat valve (d_v) diameter of 31.5 mm and outer of 34.5 mm, with bore of 79.5 mm and a stroke of 86 mm. The compression ratio is 18:1, the maximum intake valve lift is 8.1 mm and the entire intake process occurs along a crankshaft angle interval of 240°.

The experimental measures were made according the methodology described in Favero (2006) and Heywood (1988), obtaining the discharge and swirl coefficients. The discharge coefficient for a certain valve lift, C_{Dl} , is a relation between the real air flow rate through the intake valve (\dot{m}_l) and the hypothetical flow rate obtained in an isentropic expansion though the same face area ($\pi d_v^2 / 4$), for an expansion ratio outlet pressure (p_{out}) and stagnation (inlet) pressure (p_o). A global coefficient, C_D , is obtaining by integration along the crankshaft angle, as follows:

$$C_D = \frac{\int_{IVO}^{IVC} C_{Dl} d\theta}{IVC - IVO} \quad (1)$$

where θ is a crankshaft angular position, IVO is the intake valve angle opening and IVC is the intake valve angle closing.

For the present engine the obtained global coefficients are $C_D = 0.349$ and, with an estimated experimental error of 4%.

3. NUMERICAL METHODOLOGY

The computation results presented in this paper were obtained with the commercial CFD code Fluent 6.3, by using the Standard and *RNG* $k-\varepsilon$ turbulence models. All two models have similar forms, with transport equations for k and ε . The major differences in the models are the methodology for calculating turbulent viscosity, turbulent Prandtl numbers governing the turbulent diffusion of k and ε , and the generation and destruction terms in the ε equation (Fluent 2007).

The standard $k-\varepsilon$ model is a semi-empirical model based on model transport equations for the turbulence kinetic energy (k) and its dissipation rate (ε). The model transport equation for k is derived from the exact equation, while the model transport equation for ε was obtained using physical reasoning and bears little resemblance to its mathematically exact counterpart. In the derivation of the $k-\varepsilon$ model, it was assumed that the flow is fully turbulent, and the effects of molecular viscosity are negligible. The standard $k-\varepsilon$ model is therefore valid only for fully turbulent flows. The model constants have the following default values: $C_{1\varepsilon} = 1.44$; $C_{2\varepsilon} = 1.92$; $C_\mu = 0.09$, $\sigma_k = 1.0$ and $\sigma_\varepsilon = 1.3$ (Fluent 2007).

The *RNG* based $k-\varepsilon$ turbulence model is derived from the instantaneous Navier-Stokes equations, using a mathematical technique called “renormalization group” (*RNG*). The analytical derivation results in a model with constants different from those in the standard $k-\varepsilon$ model, and additional terms and functions in the transport equations for k and ε . The model constants have the following default values: $C_{1\varepsilon} = 1.42$; $C_{2\varepsilon} = 1.68$; $C_\mu = 0.0845$ (Fluent 2007).

The mesh independence study arrived in submillimeter meshes with 123,000, 523,000 and 1,028,000 cells, including a subsurface of 0.02 mm to assure an adequate wall treatment. For the High-Reynolds approach turbulence models the subsurface has 3 layers, non linearly distributed, starting from 0.005 to 0.02 mm in order to obtain dimensionless distance from the wall $y^+ < 2.3$. All computations are performed in double precision.

User defined unstructured tetra-prism meshes, with 523,000 cells, and maximum global element size of 3 mm, and 3 layers as described above, are employed as showed in the Figure 1. The convergence criteria used for residuals was in the range of 10^{-5} .

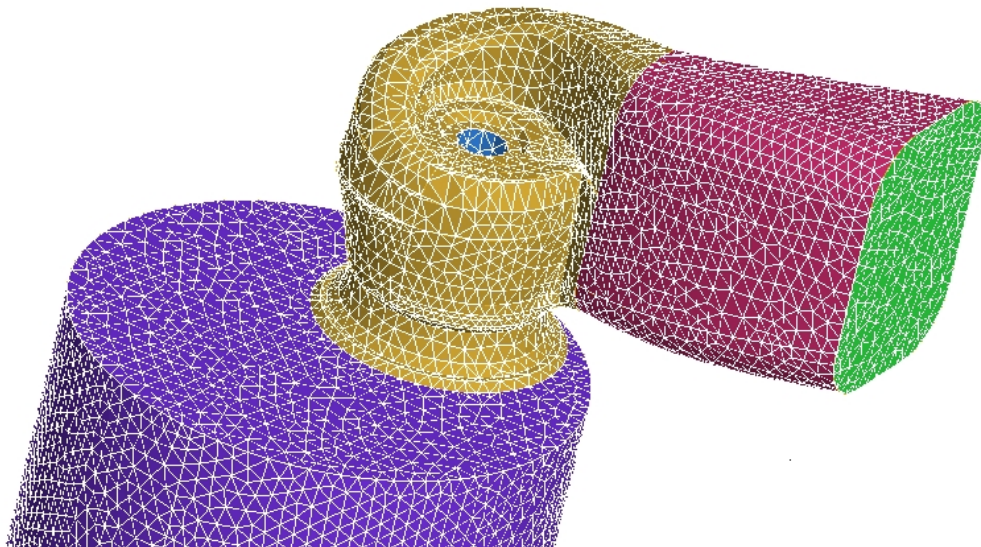


Figure 1: Unstructured tetra-prism cells mesh

The Figure 3 shows the density of the mesh with refinement next to wall, on section B-B, in the seat valve region.

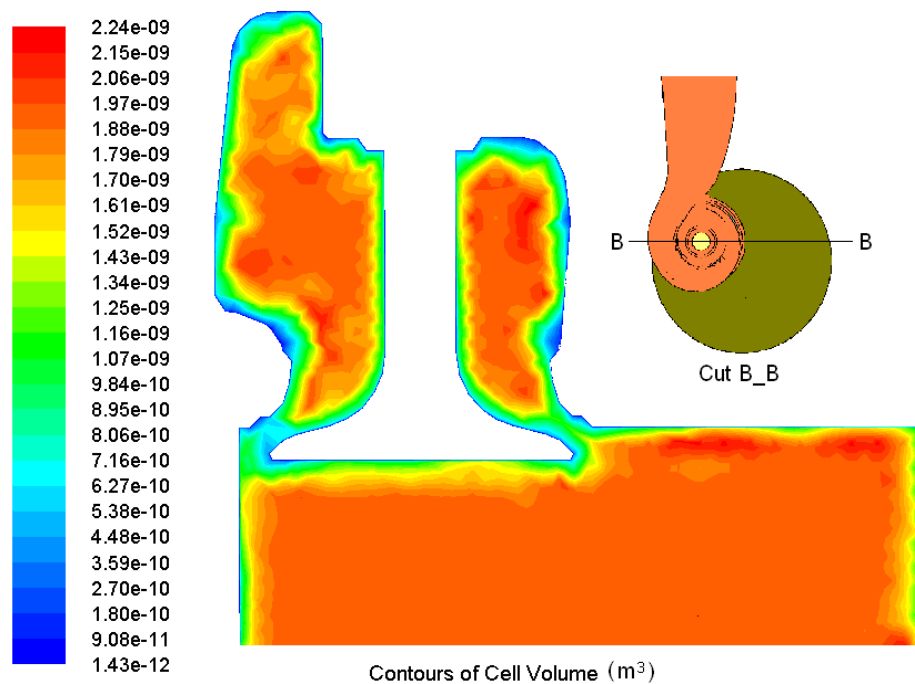


Figure 2: Mesh refinement in order to capture higher gradients

To better understand the characteristics of the phenomenon, starting from the atmospheric pressure at the inlet, were simulated expansions for 0.75 and 0.88 bar. For all cases the turbulence boundary conditions are turbulence intensity of 0.05 and length scale of 0.0035 m, as a consequence of the flow and geometrical characteristics. The pressure-velocity coupling is solved through the SIMPLEC algorithm (Patankar, 1972). The enthalpy equation is also solved, and the air is treated as a perfect gas.

4. VALIDATION OF THE NUMERICAL SIMULATIONS

For the calculation of the discharge coefficient for a certain valve lift (C_{Dl}), in the case of a non-choked flow, caused by the expansion ratio p_{out}/p_o , according to Heywood (1988),

$$C_{DI} = \frac{\dot{m}_l}{\frac{\pi d_v^2}{4} \frac{p_o}{(RT_o)^{1/2}} \left(\frac{p_{out}}{p_o} \right)^{1/k} \left\{ \frac{2k}{k-1} \left[1 - \left(\frac{p_{out}}{p_o} \right)^{(k-1)/k} \right] \right\}^{1/2}} \quad (2)$$

where \dot{m}_l is obtained from the numerical solution, or experimentally. R is the gas (air) constant, T_o the stagnation (inlet) absolute temperature and k the specific heat ratio.

As a first step, aiming to validate the present numerical implementation, simulations were done reproducing the parameters used in the CRF experimental apparatus (Fiat Research Center, 1982 and 1983): $p_o = 1.1$ atm, $p_{out} = 1$ atm, $T_o = 293$ K. The turbulence models used in this case were the Standard $k-\varepsilon$ High Reynolds. Standard near wall treatment, and the RNG , standard wall function, with default coefficients, according Fluent (2007): $C_{1\varepsilon} = 1.42$; $C_{2\varepsilon} = 1.68$; $C_\mu = 0.0845$. It is applied the Second Order Upwind. The results are described in the Tab.1, that presents the values gotten with Fluent 6.3 in the present work, and that obtained by Baratta et al. (2008), with the Star_CD 3.26.

Table 1: Simulation's results for $p_o = 1.1$ atm, $p_{out} = 1$ atm, $T_o = 293$ K

Turbulence model	Intake valve lift [mm]	Fluent 6.3		Star_CD 3.26	
		\dot{m}_l [kg/s]	C_{DI}	Diff scheme	C_{DI}
$k-\varepsilon$ High Reynolds Std wall function	1.00	0.011688	0.0963	LUD Bf 0.6	0.0966
	4.30	0.042052	0.347		0.355
	7.50	0.053491	0.441		0.442
$k-\varepsilon$ RNG Std wall funct. Modified coefficients	1.00	0.011816	0.0974	Bf 0.6	0.104
	4.30	0.042326	0.349		0.378
	7.50	0.052734	0.435		0.455

A good agreement is verified among the software, where the biggest difference occurs in the lift of 4.3 mm, for the model $k-\varepsilon$ RNG ; about 8.3%.

The numerical integrations, defined in the Eq. (1) and Eq. (2), are done considering a half symmetrical part (120°) of the valve lift curve of the present engine (Fiat Research Center, 1982 and Favero 2006), according the Tab.2.

Table 2: Angular interval for the numerical integrations corresponding to each intake valve lift

Intake valve lift [mm]	Angular interval $\Delta\theta$ [°]
1.00	18
4.30	49
7.50	53

The results of each integration, and a comparison among experimental and the results obtained by Star_CD (Baratta et al., 2008) and Fluent are shown in the Tab. 3.

Table 3: Numerical and experimental global results

	Case	C_D
	Experimental; CRF (1982, 1983) (4% of accuracy)	0.372
Fluent	Numerical simulation with $k-\varepsilon$ High Reynolds Standard wall function	0.349
	$k-\varepsilon$ RNG Std wall function	0.349
Star_CD	Numerical simulation with $k-\varepsilon$ High Reynolds Cubic Standard wall function	0.355
	$k-\varepsilon$ RNG Std wall funct. Modified coefficients	0.371

It is verified in table 3 that Fluent's results are more distant of the experimental ones. However the results gotten with the Fluent are coherent, since the percentile difference, if compared with the experimental data, is of - 6%.

5. COMPUTATIONAL RESULTS

The Figure 3 shows the velocity vectors on section A-A of the swirl generator intake port, arriving in the subsurface of 0.02 mm, containing 3 layers non-linearly distributed. It is detected a large recirculation flow, caused by the valve rod downstream low pressure. This large scale phenomenon is detected by all turbulence models and differencing schemes tested, for all valve lifts. It seems to be an intrinsic problem of the shallow ramp helical type swirl generator, and a potential cause for a reduction of discharge coefficient.

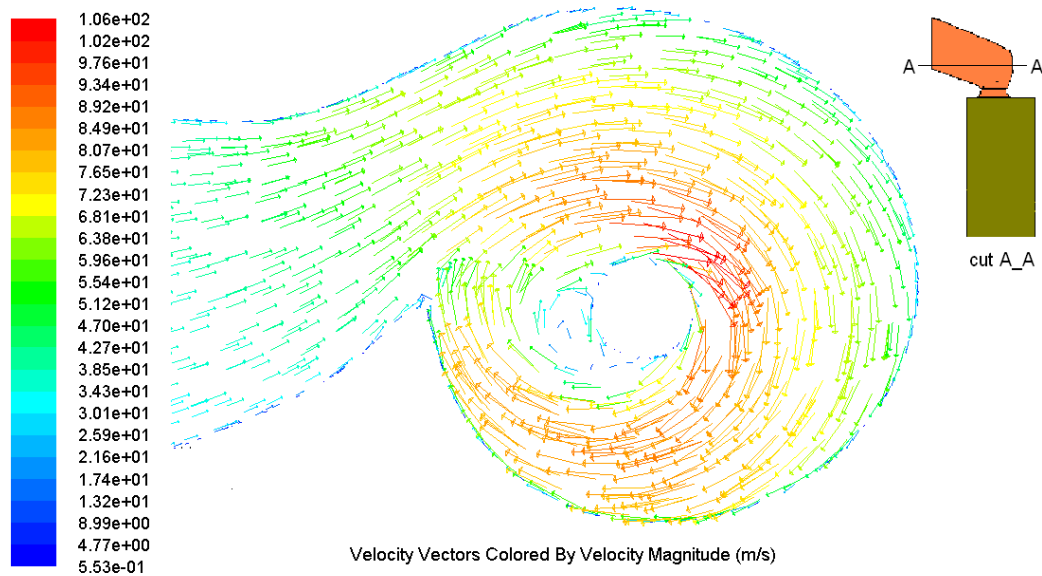


Figure 3. Velocity vectors on the cut A-A, swirl generator intake port

The Figure 4 shows the velocity vectors on section B-B, in the seat valve region. Valve lift 4.3 mm, $p_{out}/p_o = 1.0/0.88$ bar.

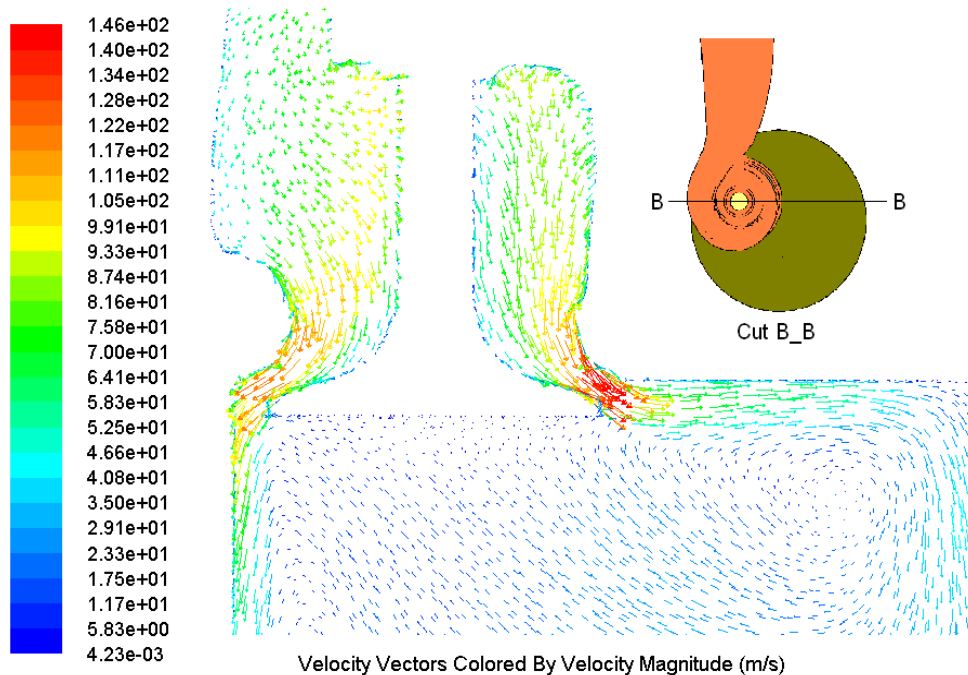


Figure 4. Velocity vectors on the cut B-B, seat valve region

Because the face area restriction, this is the point of higher velocities and friction. Indeed, this restriction causes almost all of the pressures losses of the expansion. It is also shown the annular helical jet, causing a large recirculation pattern inside de cylinder.

The Figure 5 shows velocity vectors on cut C-C, in the middle of cylinder high ($Y = 80 \text{ mm} = 1B$), for valve lift 4.3 mm and $p_{out}/p_o = 1.0/0.75 \text{ bar}$. As the intake valve is not localized at the center of the cylinder, the produced swirl is not centralized also, creating a general pattern of two macro vortices. A principal, directly generated by the helical intake port, and a secondary, induced by the former.

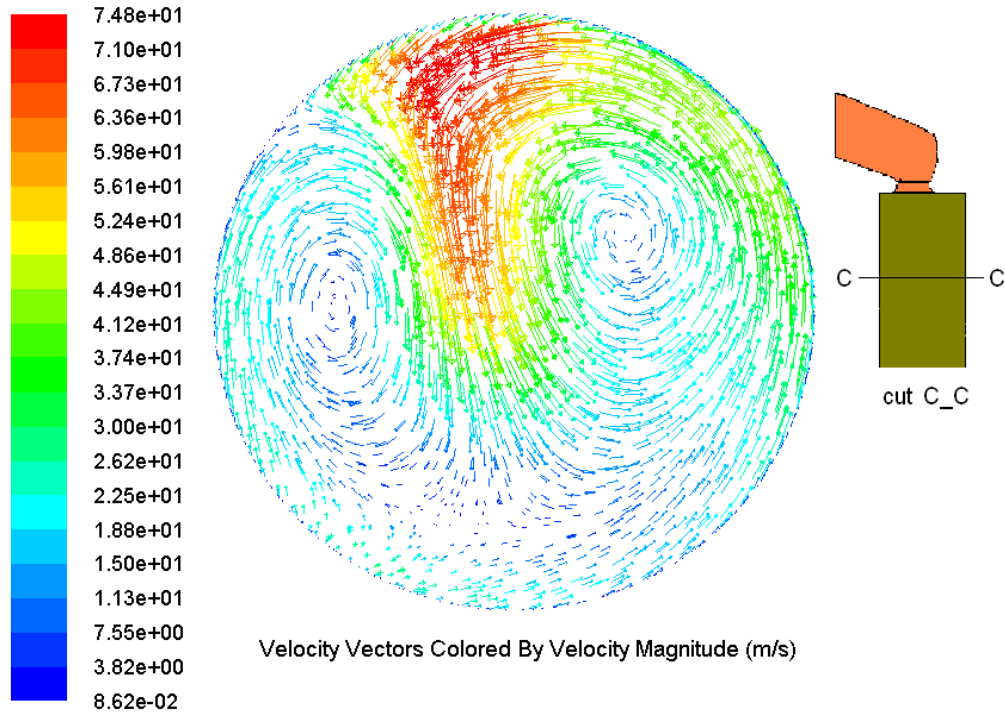


Figure 5. Velocity vectors on the cut C_C, seat valve region

6. OTHER BOUNDARY CONDITION VALUES INVESTIGATE WITH FLUENT AND COMPARED WITH STAR_CD

The tables 4, 5, 6 show comparison between results obtained from the Star_CD and of the Fluent for valve lifts of 1.0 , 4.3 and 7.5 mm . The $p_o = 1.0 \text{ bar}$, and the in-cylinder suction pressure, p_{out} , is taken 0.88 and 0.75 bar . In the Fluent it is applied a second order accurate differencing scheme, based on a corrected upwind, called second order upwind. In the Star_CD the first order upwind (UD) and also the second order linear upwind (LUD) are applied, with blending factor (bf) of 0.6 . Regarding the $k-\epsilon$ High Reynolds turbulence model, the Fluent uses a linear one, instead in the Star_CD it is applied a cubic one.

Table 4. Air mass flow rate through the intake valve and discharge coefficient for a lift of 1.0 mm

Turbulence model	p_{out}/p_o	Star_CD 3.26			Fluent 6.3		Star_CD / Fluent [%]
		Diff scheme	\dot{m}_l [kg/s]	C_{Dl}	\dot{m}_l [kg/s]	C_{Dl}	
$k-\epsilon$ High Reynolds Std wall function	0.88/1.0	UD	0.01170	0.0952	0.01083	0.0881	8.1
$k-\epsilon$ RNG Std, wall function Std coefficients		LUDbf 0.6	0.01260	0.1025	0.01151	0.0937	9.4
$k-\epsilon$ High Reynolds Std wall function	0.75/1.0	UD	0.01493	0.0919	0.01342	0.0825	11.4
$k-\epsilon$ RNG Std, wall function Std coefficients			-	-	0.01391	0.0855	-

Table 5. Air mass flow rate through the intake valve and discharge coefficient for a lift of 4.3 mm

Turbulence model	p_{out}/p_o	Star_CD 3.26			Fluent 6.3		Star_CD / Fluent [%]
		Diff scheme	\dot{m}_l [kg/s]	C_{DI}	\dot{m}_l [kg/s]	C_{DI}	
$k-\varepsilon$ High Reynolds Std wall function	0.88/1.0	UD	0.04343	0.353	0.04228	0.344	2.6
$k-\varepsilon$ RNG Std, wall function Std coefficients		LUDbf 0.6	0.04621	0.376	0.04389	0.357	5.3
$k-\varepsilon$ High Reynolds Std wall function	0.75/1.0	UD	0.05810	0.357	0.05578	0.343	4.1
$k-\varepsilon$ RNG Std, wall function Std coefficients			-	-	0.05836	0.359	-

Table 6. Air mass flow rate through the intake valve and discharge coefficient for a lift of 7.5 mm

Turbulence model	p_{out}/p_o	Star_CD 3.26			Fluent 6.3		Star_CD / Fluent [%]
		Diff scheme	\dot{m}_l [kg/s]	C_{DI}	\dot{m}_l [kg/s]	C_{DI}	
$k-\varepsilon$ High Reynolds Std wall function	0.88/1.0	UD	0.05610	0.457	0.05347	0.435	5.0
$k-\varepsilon$ RNG Std, wall function Std coefficients		LUDbf 0.6	0.05508	0.448	0.05233	0.426	5.2
$k-\varepsilon$ High Reynolds Std wall function	0.75/1.0	UD	0.07693	0.473	0.07174	0.441	7.2
$k-\varepsilon$ RNG Std, wall function Std coefficients				-	0.07003	0.431	-

Table 7. C_{DI} integrated results for $p_o = 1.0$ bar, $p_{out} = 0.88$ and 0.75 bar

Turbulence model	p_{out}/p_o	C_D Star_CD	C_D Fluent	Star_CD / Fluent [%]
$k-\varepsilon$ High Reynolds Std wall function	0.88/1.0	0.360	0.346	4.0
	0.75/1.0	0.369	0.347	6.3
$k-\varepsilon$ RNG– Std wall function Std coefficients	0.88/1.0	0.367	0.348	5.5
	0.75/1.0	-	0.350	-

From the tables above it can be seen that Star_CD 3.26 gives major air mass flow than the Fluent 6.3, for all the lifts solved and expansion ratios. Consequently the integrated results follow the same tendency. The turbulence models, and also the differencing schemes tested do not change this behavior. The bigger differences occur for the lift of 1.0 mm, where the stresses are relatively major due to the severe restriction cause by the intake valve. This region, followed by the flow separation backward the valve, requires a lot of the turbulent models.

Keeping attention on the same software (Star_CD or Fluent), for the same expansion ratios and valve lifts, it is possible to verify differences of the same order between their differencing schemes, as could be expected. Baratta et al. (2008) reported the same behavior.

7. CONCLUSIONS

The 3D turbulent, compressible flow in an internal combustion engine intake is solved, for three different valve lifts and expansion ratios. Comparisons between numerical and experimental data showed good agreement.

One verifies that the discharge coefficient for each valve lift increases with increasing lift, as expected. Also the air flow rate through the intake valve varies with pressure ratio, increasing as the pressure ratio increases.

For the expansion ratio p_{out}/p_o of 1.0/1.1, the $k-\epsilon$ High Reynolds model and $k-\epsilon$ RNG presented similar values in Fluent, for the global discharge coefficient, however distant of - 6% of the experimental data.

The Star_CD, for the differencing schemes, mesh and turbulence models tested presented discharge coefficients results a little greater than Fluent.

For the expansion ratio p_{out}/p_o of 0.88/1.0 and 0.75/1.0, the relationship between Star_CD and Fluent is about 5% for the discharge coefficient.

For all the models investigated, the presence of recirculations in the port and in-cylinder are detected.

In the case of a practical application, considering that the objective is not the comparison between softwares, it should be applied the second order LUD differencing scheme, requiring a global residual tolerance equal or less than $2.E-5$, for all the solved variables. This kind of intake system, considering its 3D turbulent complex compressive flow, requires a submillimeter mesh, with the necessary subsurface, arriving in a half million cells.

8. ACKNOWLEDGMENTS

The authors thank the financial support from CAPES-Brazil through a post-doctorate scholarship grant to Vielmo, H.A.

9. REFERENCES

- Baratta, M., Catania, A.E., Spessa, E., and Liu, R.L., 2003. "Multidimensional Predictions of In-Cylinder Turbulent Flows: Contribution to the Assessment of $k-\epsilon$ Turbulence Model Variants for Bowl-In-Piston Engines". ASME J. of Eng. Gas Turbines Power, 127, pp. 883-896.
- Baratta, M., Catania, A.E., Pesce, F.C., Spessa, E., Vielmo, H.A. 2008. "Numerical Analysis of a High Swirl-Generating Helical Intake Port for Diesel Engines". Submitted to the ENCIT 2008.
- Bianchi, G.M., Cantore, G. and Fontanesi, S., 2002. "Turbulence Modeling in CFD Simulation of ICE Intake Flows: The Discharge Coefficient Prediction". SAE Paper N° 2002-01-1118.
- Bianchi, G.M., Cantore, G., Parmeggiani, P. and Michelassi, V, 2002. "On Application of Nonlinear $k-\epsilon$ Models for Internal Combustion Engine Flows". Transactions of the ASME vol. 124, pp. 668-677.
- Bianchi, G.M., Fontanesi, S., 2003. "On the Applications of Low-Reynolds Cubic $k-\epsilon$ Turbulence Models in 3D Simulations of ICE Intake Flows". SAE Paper N° 2003-01-0003.
- Favero, F., 2006. "Tecniche di Modellazione e di Analisi Numerica per lo Studio del Moto della Carica in Camera di Combustione e loro Applicazione ad un Motore Diesel ad Elevato Swirl". Thesis, IC Engines Advanced Lab, Politecnico di Torino, Italy, (in italian).
- Fiat Research Center; Consiglio Nazionale delle Ricerche, 1982. "Motore Monocilindro Diesel con Distribuzione a 2 Valvole e Protezioni Termiche Camera di Combustione". Contract N° 82.00047.93 (in italian).
- Fiat Research Center; Consiglio Nazionale delle Ricerche, 1983. "Metodologia per la Caratterizzazione dei Condotti di Aspirazione Motori in Flusso Stazionario". Contract N° 82.00047.93 (in italian).
- Fluent 6.3 User Guides, 2007.
- Heywood, J.B., 1988. "Internal Combustion Engines". McGraw-Hill Inc.
- Patankar, S.V. and Spalding, D.B., 1972. "A Calculation Procedure for Heat, Mass and Momentum Transfer in Three-Dimensional Parabolic Flows". Int. J. Heat Mass Transfer, 15, pp. 1787-1806.

10. RESPONSIBILITY NOTICE

The authors are the only responsible for the printed material included in this paper.